STEADY STATE MODELING OF A FIRE TUBE BOILER

Wim Beyne*[1,2] , Dieter Daenens[1], Bernd Ameel[1,2], Marnix Van Belleghem[3], Steven Lecompte[1,2], Michel De Paepe[1,2]
* Author for correspondence
[1] Department of Flow, Heat and Combustion Mechanics, Ghent University, Sint-Pietersnieuwstraat 41, B-9000 Ghent, Belgium
[2] Flanders Make, the strategic research centre for the manufacturing industry, Campus Arenberg Celestijnenlaan 300 - bus 4027 B-3001 Heverlee, Belgium
[3] Deconinck-Wanson, Legen Heirweg 43 9890 Gavere Belgium
E-mail: wim.beyne@ugent.be

ABSTRACT

Manufacturers increasingly strive to customize fire tube boiler designs to specific needs. A comprehensive thermal design model is therefore necessary. In this article a steady state thermal model based on the plug flow furnace model and the ε-NTU method is presented. The model includes the turn boxes which other authors neglect. The steady state model furthermore allows optimizing the boiler designs. It is used to analyze the gas temperature along the flow length. Secondly, the article compares a plug flow furnace model, the ε- NTU method with and without radiation. The ε- NTU with radiation allows decreasing the number of control volumes while retaining accuracy. Additionally the effect of the turn boxes is investigated.

INTRODUCTION

Fire tube boilers provide steam for a wide range of applications in the process industry. To develop new boiler designs, without an extensive experimental campaign, a comprehensive thermal design model is necessary. Boilers and heat exchangers have to satisfy steady state performance requirements such as operating pressure and steam production rates [1]. These requirements can be evaluated with a steady state thermal model.

Literature on steady state models is however very scarce. In literature, three steady state thermal models for fire tube boilers can be found [2-4]. They are based on a discretization of the boiler in three zones: gas zone, metal zone and water/steam zone. All three models focus on the gas to metal heat transfer in the fire tubes. Only the models by Rahmani et al. [3, 4] do not a priori require calibration with experimental results and are thus suitable for design purposes. The most recent model [4] applies the plug flow furnace model [5] in the furnace and tube passes. The turn boxes are neglected.

This paper develops a steady state thermal model, based on general experimental correlations and conservation laws. The model allows preliminary design calculations and operational robustness calculations. The model accounts for the effect of turn boxes, which were previously omitted in literature. Furthermore, the importance of radiation modelling in the tube passes is compared using two alternatives to the plug flow model in the tube passes.

NOMENCLATURE

A_{mi}	[m²]	Metal inner surface area
A_t	[m²]	Turn box outer surface area
g_{rad}	[m²]	Total radiative heat transfer factor
h	[W/(m²K)]	Convective heat transfer coefficient
NTU	[-]	Number of Transfer Units
$\dot{Q}_{gm}$	[W]	Heat transfer from gas to metal
$\dot{Q}_l$	[W]	Heat loss through the non-submerged turn box
R	[K/W]	Heat transfer resistance
T_{amb}	[K]	Ambient temperature
T_g	[K]	Gas temperature
T_{mi}	[K]	Inner metal temperature
T_{to}	[K]	Turn box outer temperature
Special characters		
σ	[W/(m²K⁴)]	Stefan Boltzmann constant
ε	[-]	Effectiveness
ε_g	[-]	Emissivity gas
ε_t	[-]	Emissivity outside turn box wall
ε_m	[-]	Emissivity metal

STEADY STATE MODEL

Three main performance parameters of a fire tube boiler are the attainable steam production at a given operating pressure, the thermal efficiency and the local wall temperature. A thermal design model should thus provide estimates for these performance parameters.

The steady state model in this work is based on a three flue gas pass design with one submerged turn box, as shown in Figure 1. The modelling approach is similar to the approach of Rahmani and Trabelsi [4], but includes the turn boxes. The steam boiler is considered as several heat exchangers in series, submerged in a uniform, saturated water volume. A two-phase water/steam zone, metal zone and gas zone are discerned. The model is set up by determining the state of each zone and the heat transfer from one zone to another.

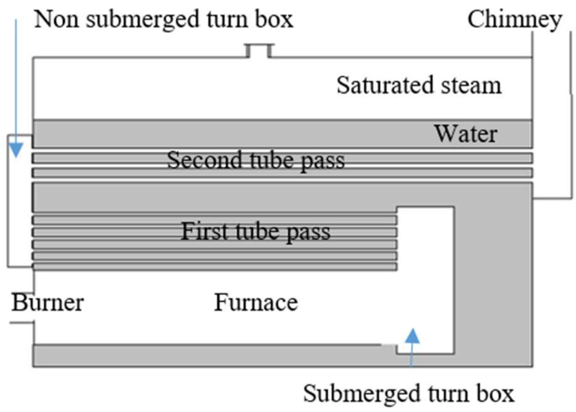

Figure 1: Three pass fire tube boiler design with submerged turn box.

The two-phase water/steam zone is modelled by a single control volume. Thermodynamic equilibrium between the phases is assumed. The evaporation pressure is assumed to be controlled to the adequate level for the application. The steam production is equal to the ratio of the total heat transfer from the metal zone to the water zone to heat required to evaporate the incoming feed water.

The gas zones are divided in multiple control volumes for the furnace and tube passes and one control volume for the turn boxes. Expressing the conservation of mass, energy and momentum on the control volumes results in a set of equations which determines the gas and metal zone states. To solve the resulting set of equations, the heat transfer from one zone to another and the heat release by combustion is determined.

HEAT TRANSFER

The heat release by combustion is modelled by an exponential release law as is done by Gutiérrez [6]. Rahmani and Trabelsi use a parabolic release law [4]. The release law should be fitted to the burner installed in the fire tube boiler. The heat transfer rate $\dot{Q}_{gm}$ between the gas and metal zone is modelled by the plug flow furnace model as shown in Equation 1.

$$\dot{Q}_{gm} = g_{rad}\, \sigma \left(T_g - T_{mi}\right) + h\, A_{mi} \left(T_g - T_{mi}\right) \qquad (1)$$

g_{rad} denotes the total radiative heat transfer coefficient. Under the assumption of an infinitely long tube without axial radiation it can be written as Equation 2 [5].

$$g_{rad} = A_{mi} \left(\frac{1-\varepsilon_m}{\varepsilon_m} + \frac{1}{\varepsilon_g}\right)^{-1} \qquad (2)$$

A_{mi} is the inner metal surface area, ε_m the metal emissivity and ε_g the gas emissivity. The gas emissivity is determined using a polynomial approach by Taylor and Forster [7]. The correlation is valid between 1200 and 2400 K and takes both the gas temperature, the geometry of the enclosure and the partial pressure of CO_2 and H_2O into account. Outside this range, a correlation by Talmor is used [8] taking only the combustion gas composition into account. The emissivity correlations have large uncertainties up to 35 % [9]. However the uncertainty on the emissivity and determination of g_{rad} resulted in an uncertainty on the total heat transfer of less than 0.2 %.

The inner metal wall temperature T_{mi} is determined by an equivalent thermal resistance network, as used by Huang et al. [2]. The thermal resistance on the water side is determined using the nucleate boiling correlation of Cornwell [10]. In the tube bundles, a correction by Gorenflo [6] is made for the effect of closely packed tubes. The convective heat transfer coefficient is determined by the Gnielinski correlation [11].

Equation 1 is comprised of a radiative and a convective part. Radiation is less important in the tube passes and is therefore often neglected [1]. If convection is dominant, convection dedicated methods such as the ε-NTU method [5] can be applied. If radiation is important but not dominant, radiative heat transfer can be included by linearizing the radiative heat transfer as a function of the temperature difference.

The ε-NTU method needs less control volumes compared to the plug flow furnace model to accurately predict heat transfer. In this work, three models are made and compared. One model uses the plug flow furnace model in the tube passes (further called the PF variant), another model uses the ε-NTU method in the tube passes (further called the NTU variant), a third model uses the ε-NTU method in the tube passes but includes radiation (NTURAD). The results for all three models are compared in the results section.

The turn boxes are analysed using similar equations as for a tube pass, but with adapted geometrical parameters. The flow pattern inside the turn boxes complicates the definition of the convective heat transfer coefficient h. However, jet impingement on the back plate is expected to be dominant over the convection induced by the turned flow. Therefore, the convective heat transfer coefficient is determined from correlations of jet impingement [12]. The metal temperature and waterside heat transfer are treated the same as for the furnace and tube passes.

The non-submerged turn box results in radiation losses to the ambient. Since the heat transfer coefficient on the flue gas side is larger (jet impingement, forced convection and radiation) than on the ambient side (radiation and natural convection at lower temperatures), the thermal resistance on the gas side is neglected. The inner wall temperature of the non-submerged turn box is thus taken as the flue gas temperature. The heat loss to the ambient is determined by Equation 3.

$$\dot{Q}_l = A_t\, \varepsilon_t\, \sigma \left(T_{to}^4 - T_{amb}^4\right) + \frac{1}{R} \left(T_g - T_{amb}\right) \qquad (3)$$

$\dot{Q}_l$ denotes the heat loss to the environment, ε_t the emissivity of the outside of the turn box, A_t the surface area of the turn box, R the conductive and convective heat transfer resistance, T_{to} the turn box outside temperature and T_a the ambient temperature. Once the heat loss is known, the turn box outside temperature can be determined by solving the resistance circuit of the turn box walls. The loss is determined by iterating between Equation 3 and the determination of T_{to}.

RESULTS

The simulations are based on one of the boilers described in the measurement reports. The boiler characteristics are given in Table 1.

Power	1 252 kW
Steam production	0.56 kg/s (2 ton/h)
Steam content	0.947 m^3
Water content	4.049 m^3
Length	3.75 m
Width	2.015 m
Height	2.42 m

Table 1 Boiler characteristics.

The steady state model allows estimating key performance indicators, such as the obtainable steam production and the chimney gas temperature. Secondly, it allows calculating local heat transfer parameters and assessing different design options. The output of the model is studied in the following section.

Temperature and heat transfer profiles

Figure 2 shows the temperature as a function of the flow length calculated with the plug flow model. The gas and metal centreline temperature profile are similar to the results of Rahmani and Trabelsi [4]. The gas temperature first rises as a result of the combustion. It reaches a maximum when the heat transfer from the gas to the metal equals the transfer to the gas from the combustion. In the tube passes, the gas temperature resembles a purely convective profile, which indicates the importance of convection over radiation. The water/steam mixture is modelled as one saturated control volume with a fixed pressure. The water temperature is therefore constant. The metal temperature at the centreline is closer to the water temperature than the gas temperature. This is the result of the higher heat transfer resistance on the gas side.

The grey vertical dashed lines represent the position of the turn boxes. The temperature curve shows a large temperature jump in the first turn box. This indicates the importance of including the turn box in the model.

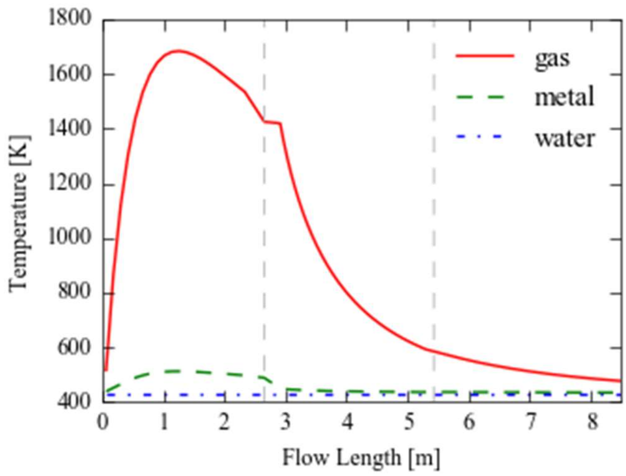

Figure 2 Temperature and pressure as a function of the axial distance; (a) temperature profile, (b) pressure profile; grey lines represent turn boxes.

The radiative and the convective fraction of the heat transfer rate are shown in Figure 3. The changing importance of radiation or convection is attributed to two flow properties. Firstly, a high local gas temperature increases the radiative fraction. After all, radiation is proportional to temperature to the fourth power while convection is linear with respect to the temperature difference. Secondly, a high gas velocity increases the convective heat transfer by an increase in the convection heat transfer coefficient. The gas velocity is influenced both by the gas temperature and by the gas through flow section. The density variation along the flow length is within 70 % of the maximum density. However, changes of geometry like going from the furnace to the tube passes reduce the flow section by as much as 85 %, resulting in a large increase in the local velocity. The effect of the change in geometry is therefore dominant over the effect of the decreasing gas temperature on the convective heat transfer. The changes in the geometry are responsible for the apparent discontinuities observed in Figure 3.

Radiation is dominant throughout the furnace and submerged turn box. Both the furnace and turn box are characterized by a high gas temperature and low local gas velocities. The radiative fraction peaks in the turn box. At the turn box, convection is estimated as jet impingement on the back wall, while radiation is calculated on all the turn box surfaces namely the cylinders mantle, top and bottom plate. The convective surface area is about 40 % of the radiative surface area. Therefore the radiative relative fraction peaks in the submerged turn box. The radiative fraction reduces in the tube passes, due to the decrease of the gas temperature.

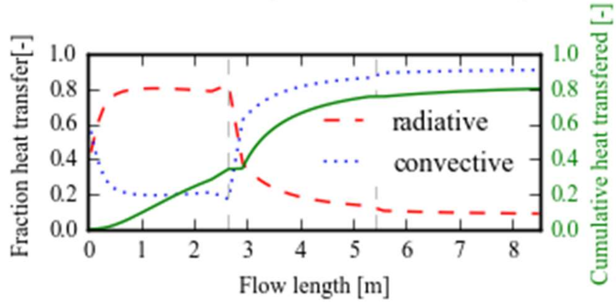

Figure 3 Fraction of heat transfer by radiation, convection and the cumulative heat transferred along the axial length at nominal load.

The green curve on Figure 3 shows the cumulative heat transferred. The heat transferred is referenced to the total combustion heat. Note that most of the heat is transferred in the furnace and first tube pass. The second tube pass only increases the efficiency by a couple of percentage points. The submerged turn box contributes about 6 % to the total heat transferred.

Model comparison

Three alternative models are compared: the plug flow model (PF), the NTU model (NTU) without radiation and the NTU model with radiation (NTURAD). The models' performance are compared both at nominal firing rate and at a reduced firing rate of 40 %.

The calculated thermal efficiency of the fire tube boiler and the chimney flue gas temperature are a first measure to compare the three model variants. The PF and NTURAD model calculate the same efficiency (up to 0.1 %) and the same chimney temperature (up to 1 K) both at nominal and at reduced firing rate. The calculated efficiency according to the NTU model differs by only 1.1 % at nominal firing rate and 0.9 % at a reduced firing rate. The temperature difference is 21 K at nominal and 42 K at reduced firing rate.

There is a large difference between the NTU model performance for nominal and reduced firing rates. The maximum temperature deviation and root mean square deviation are about 60 K higher at reduced firing rate than at nominal firing rate for the NTU model. This is inverse to what would be expected from the higher gas temperatures at nominal firing rate. At reduced firing rate, the radiative fraction in the tube passes is however increased. As a result, the first tube pass heat transfer is underestimated by 7 % by the NTU model. Due to increased gas temperature calculated at the start of the second tube pass, the heat transfer of the second tube pass is overestimated by 26 % by the NTU model.

The worse performance of the NTU variant compared to the PF model and the NTURAD model is visualized by Figure 4 and Figure 5. Figures 4 and 5 show the temperature profiles in the first tube pass at nominal firing rate and at reduced firing rate. All three models start at the same temperature since the furnace and turn box model is the same. The NTU model however deviates from the other two models along the flow length. The deviation is larger at reduced firing rate (Figure 4) than at nominal firing rate (Figure 5). Neglecting radiation in the tube passes thus results in a large error on the local gas temperature.

Both the PF model and NTURAD model are capable of estimating local gas temperatures. However, less control volumes are needed for the NTURAD model to retain high accuracy compared to the PF model. Figure 6 shows the gas temperature profile for the PF model with 500 CV and 5 CV and the NTURAD model with 5CV. The NTURAD model retains its accuracy at reduced number of control volumes. As a result, using the NTURAD models allows for fewer control volumes and faster calculation times than the PF model. The presented NTURAD model thus allows a significant reduction of computational effort compared to the models found in literature.

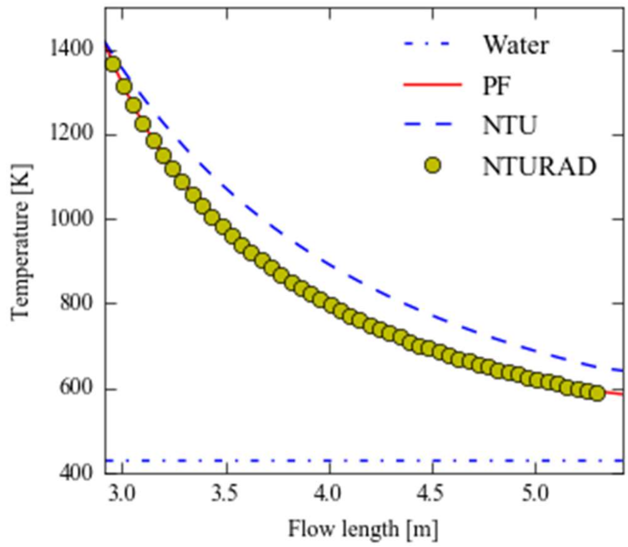

Figure 4 Temperature profile in the first tube pass for the PF, NTU and NTURAD models at nominal firing rate.

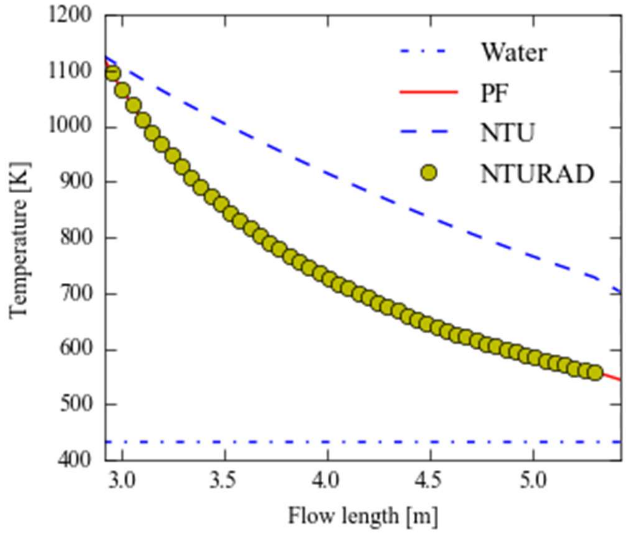

Figure 5 Temperature profile in the first tube pass for the PF, NTU and NTURAD models at low firing rate.

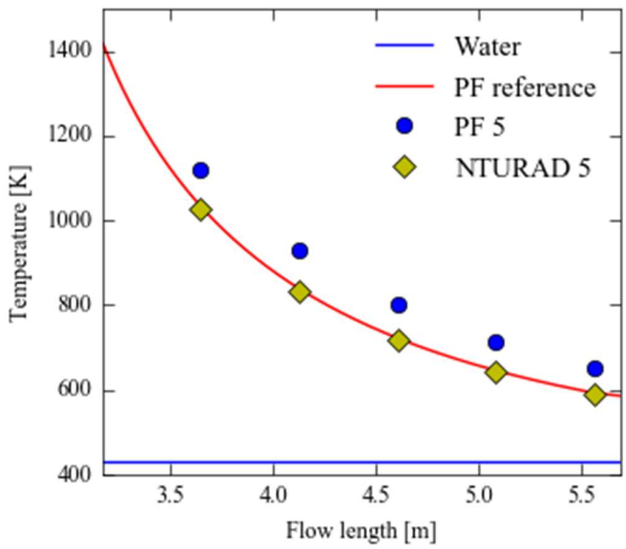

Figure 6 Temperature profile in the first tube pass for the PF model with 500 control volumes and the PF and NTURAD model with 5 control volumes.

CONCLUSION

To optimize boiler designs for a specific goal, a rigorous thermal model of a boiler is required. The fire tube boiler is modelled as a series of heat exchanges submerged in a saturated water volume. The furnace and turn box is modelled with a plug flow model. The turn box contributed 7 % to the total heat transferred. In the tube passes a plug flow model, an effectiveness-NTU model including radiation and an effectiveness-NTU model without radiation for the tube passes were compared. This showed that the NTU model is not applicable at lower loads, due to the increasing importance of radiation at these loads. For firing rates equal to 40% of the nominal firing rate, the NTU model underestimated the first tube pass heat transfer by 7 % and overestimated the second tube pass by 26 %. The NTU model including radiation obtained good results and was less sensitive to reducing the number of control volumes than the PF model. The model allows reducing oversizing of custom made boilers while fitting the users' needs. Both capital and expenditure cost can thus be decreased.

REFERENCES

[1] A. Rahmani, T. Bouchami, S. Bélaïd, A. Bousbia-Salah, and M. H. Boulheouchat, "Assessment of boiler tubes overheating mechanisms during a postulated loss of feedwater accident," *Applied Thermal Engineering,* vol. 29, pp. 501-508, 2 2009.

[2] B. J. Huang, R. H. Yen, and W. S. Shyu, "A Steady-State Thermal Performance Model of Fire-Tube Shell Boilers," *Journal of Engineering for Gas Turbines and Power,* vol. 110, pp. 173-179, 1988.

[3] A. Rahmani and A. Dahia, "Thermal-hydraulic modeling of the steady-state operating conditions of a fire-tube boiler," *Nuclear Technology and Radiation Protection,* vol. 24, pp. 29-37, 2009.

[4] A. Rahmani, "Numerical Investigation of Heat Transfer in 4-Pass Fire-Tube Boiler," *American Journal of Chemical Engineering,* vol. 2, p. 65, 2014.

[5] E. U. Schlunder, *Heat exchanger design handbook*: Hemisphere Publishing,New York, NY; None, 1983.

[6] F. J. Gutiérrez Ortiz, "Modeling of fire-tube boilers," *Applied Thermal Engineering,* vol. 31, pp. 3463-3478, 2011.

[7] P. B. Taylor and P. J. Foster, "The total emissivities of luminous and non-luminous flames," *International Journal of Heat and Mass Transfer,* vol. 17, pp. 1591-1605, 12 1974.

[8] E. Talmor, *Combustion hot spot analysis for fired process heaters*: Gulf Pub Co, 1982.

[9] N. Lallemant, A. Sayre, and R. Weber, "Evaluation of emissivity correlations for H_2O□CO_2□N_2/air mixtures and coupling with solution methods of the radiative transfer equation," *Progress in Energy and Combustion Science,* vol. 22, pp. 543-574, 1996.

[10] B. Touhami, A. Abdelkader, and T. Mohamed, "Proposal for a correlation raising the impact of the external diameter of a horizontal tube during pool boiling," *International Journal of Thermal Sciences,* vol. 84, pp. 293-299, 10 2014.

[11] V. Gnielinski, "On heat transfer in tubes," *International Journal of Heat and Mass Transfer,* vol. 63, pp. 134-140, 2013.

[12] R. Viskanta, "Heat transfer to impinging isothermal gas and flame jets," *Experimental thermal and fluid science,* vol. 6, pp. 111-134, 1993.